EVALUATION OF BIOCOMPATIBILITY AND BIOACTIVITY FOR POLYMETHYL METHACRYLATE – BIOACTIVE GLASS NANOCOMPOSITE FILMS OBTAINED BYMATRIX ASSISTED PULSED LASER EVAPORATION

Laura FLOROIAN[1], Ion MIHAILESCU[2], Felix SIMA[3], Gheorghe STANCIU[4], Bogdan SAVU[5]

Noi am evaluat rezistența la zgâriere, aderența și duritatea pentru un nou compozit: polimetil metacrilat - biosticlă (*PMMA+BG*) *depus prin tehnica evaporării laser pulsate asistate de o matrice, pe substrat de titan de grad medical, pentru aplicații în implantologie. Bioactivitatea filmelor a fost evaluată in vitro prin imersia lor în fluid uman simulat (SBF) pentru diferite perioade de timp, urmată de analize de spectrosie înînfraroşu cu transformată Fourieri de microscopie confocală cu scanare laser, pentru a determina formarea hidroxiapatitei pe suprafața bioactivă. Interacțiunea dintreosteoblaste umane şi materialul testat a fost studiată prin marcarea fluorescentă a proteinelor celulare: actina şi vinculina. Osteoblastele umane au arătat că acoperă întreaga structură, cu care interacționează puternic, ceea ce e o dovadă a biocompatibilității filmelor de PMMA+GB.*

We evaluated the scrach resistance, adherence and hardness for novel polymethyl methacrylat-bioglass (PMMA+BG) composites deposited by matrix assisted pulsed laser evaporation technique on medical titanium substrate, for applications in implantology. The bioactivity of the films was assessed in vitro by soaking the composite material films into simulated body fluid (SBF) followed by Fourier transform infrared spectrometry and confocal scanning laser microscopy analysis to determine the extent of hydroxyapatite formation on the bioactive surface. Interaction between human osteoblasts and tested material was studied by fluorescent mark of cellular proteins: actin and vinculin. The human osteoblasts were shown to cover the entirely structures with which they strongly interact and this is an evidence of the PMMA+BG films biocompatibility.

Key words: bioactive glass, matrix assisted pulsed levaporation, confocal scanning laser microscopy

[1] Assist., Transilvania University of Braşov, România, e-mail: lauraf@unitbv.ro
[2] Lasers Department, National Institute for Lasers, Plasma and Radiation Physics, Bucharest-Măgurele, Romania
[3] Lasers Department, National Institute for Lasers, Plasma and Radiation Physics, Bucharest-Măgurele, România
[4] Prof., Physics Department, University POLITEHNICA of Bucharest, Romania
[5] Center for Microscopy-Microanalysis and Information Processing, University POLITEHNICA, Bucharest România

1. Introduction

Due to the fact that many diseases/malfunctions of tissues and organs and other medical conditions cannot be healed or even treated successfully by conventional medical procedures, the field of biomaterials has developed tremendously over the last years. Healthcare consumers nowadays need increasingly more advanced devices for diagnosis and treatment. New materials and innovative procedures and protocols to speed up osseointegration and subsequent bone repair and healing are needed to be developed.

Among the biomaterials with great potential we emphasize newly formulated bioactive glasses and their composite which are capable to interact with living materials and can be used in implantology and bone repair applications. In bulk the bioactive glasses brittle so that they are used as coatings for metallic implants. Metals are mechanically suitable for load-bearing orthopedic and dental implants, but nevertheless, various problems related to corrosion, wear, and negative tissue interactions have been reported [1]. The coating of metallic implants with thin layers of bioactive material combines mechanical advantages with excellent biocompatibility. Furthermore, the coatings can protect the implants from corrosion, limiting the release of metallic ions into the body [2-5].

In this study we investigate the possibility of using bioresorbable and bioactive composite made from polymethyl methacrylate (PMMA) and bioactive glass BG for implants or prosthesis for bone restoration and dental surgery. This new material is tested from the point of view of bioactivity and of mechanical properties.

2. Materials and methods

Polymethyl methacrylate – $(C_5O_2H_8)_n$ – is the synthetic polymer of methyl methacrylate and is a transparent plastic often used as an alternative to glass because of its moderate properties, easy handling and processing and low cost.

PMMA has a density of $(1.150–1.190)\cdot10^3$ kg/m^3. This is less than half of the density of glass, and similar to that of other plastics and of human bone. PMMA has a good impact strength higher than that of glass or polystyrene. It has excellent environmental stability compared to other plastics such as polycarbonate.

Unfortunately PMMA is softer and more easily to be scratched than glass. We want to obtain scratch-resistant coatings by the addition of the bioglass particles which besides have the ability to chemically bond to both bone and soft tissue (are bioactive).

In experiments we used bioactive glasses further denoted BG that contained 56.5% SiO_2, 11% Na_2O, 3% K_2O, 15% CaO, 8.5% MgO, 6% P_2O_5 .

PMMA was dissolved in chloroform (percentageof 3% PMMA) and into this solution was introduced the bioglass (0.5%) in suspension. This mixture was freezed and maintained to a constant temperature and it served as targets in thin layer deposition which was made using the matrix assisted pulsed laser evaporation technique (MAPLE).

An excimer laser is used (KrF* at $248 \cdot 10^{-9}$ m) with $25 \cdot 10^{-9}$ s pulse width, at 10 Hz repetition rates, focused to a $16 \cdot 10^{-6}$ m^2 spot size on the target. The best regime of deposition was identified for the next conditions: 5500 J/m^2 laser fluence, 266.6 10^{-2} Pa pressure, 30°C substrate temperature, 0.03 m target-substrate distance; for the deposition of each film, we applied 12500 consecutive laser pulses. Once the chamber is evacuated, the target is cooled to 100 K temperature. Target is continuously rotated and translated during the multipulse laser irradiation in order to avoid drilling and obtain homogenous coatings.

We used chemically etched medical grade Ti as substrate, because titanium is the most popular choice for the fabrication of orthopedic implants where high strength is required thanks to its good biocompatibility and very good mechanical characteristics.

3. PMMA+BG films characterization

3.1. Mechanical characterization

For determination of the films' scratch resistance and adherence on the substrate we used nanoscratch testes. These tests were performed using nanoscratch tester CSM Instruments and were consisted of the generation of scratches with a spherical stylus with $5 \cdot 10^{-6}$ m radius, which is drawn at $0.33 \cdot 10^{-4}$ m/s constant speed across the coating-substrate system to be tested, under progressive loading at a fixed rate. Initial load was 0.0003 N and the loading rate was $3.33 \cdot 10^{-9}$ m/s. The critical load (Lc) is determined as the smallest load at which a recognisable failure occurs.

The microhardness of the investigated samples was measured by using Vicker's microhardness indenter (Shimadzu, Japan). The eyepiece on the microscope of the apparatus allowed measurements with an estimated accuracy of 0.5 mm for the indentation diagonals. At least six indentation readings were made and measured for more samples. Testing was made by load 100 g and loading time was fixed to 15 s. The measurements were carried out under normal atmospheric conditions. The Vicker's microhardness value was calculated from the following equation:

$$H_v = \frac{Ap}{d^2} \quad \text{kg/mm}^2$$

where A is a constant equal to 1854.5 takes into account the geometry of squared based diamond indenter with an angle 136° between the opposing faces, p is the applied load (g); and d is the average diagonal length (mm). The microhardness values are converted from kg/mm^2 to MPa by multiplying in a constant value 9.8 [6].

3.2. Bioactivity tests

The bioactivity of the films was assessed in vitro by soaking the composite material films into simulated body fluid (SBF) followed by FTIR spectroscopic analysis to determine the extent of hydroxyapatite formation on the bioactive surface. The SBF was prepared by the mixing sodium chloride, sodium bicarbonate, potassium chloride, potassium phosphate, calcium chloride, dibasic potassium phosphate, hydrogen chloride, sodium sulfate and tris(hydroxymethyl)aminomethane into de-ionized water, according to Kokubo prescription [7]. The obtained solution had ionic concentration equal to human plasma. Table 1 compares the ionic concentrations of SBF with that of blood plasma.

The disks coated with sintered bioactive films were tested by immersion into $25.0 \cdot 10^{-6}$ m^3 SBF preheated and maintained to 37 °C. Tests are conducted 1 day to 2 weeks after immersion by confocal scanning laser microscopy (CSLM) and Fourier transform infrared spectrometry (FTIR).

The morphological investigation process by using CSLM is based on a sequential exploration of a sample by a laser beam and on the monitoring of interaction effects between light and material for surface or spatial imaging. We used a Leica TCS SP system equipped with a He-Ne laser source ($632.8 \cdot 10^{-9}$ m) and a PL Fluotar (40X magnification, numerical aperture NA= 0.7) objective. The images were recorded in reflection mode. Data processing and displaying were performed by Leica software.

FTIR analyses were conducted using a Nicolet 380 apparatus equipped with an orbit ATR (diamond crystal), wavenumber range $(7800 - 350) \cdot 10^2$ m^{-1}, spectral resolution 40 m^{-1}, S/N ratio 20000:1. The spectra were taken in the absorbance mode.

Table 1

Comparison of ionic concentrations of SBF and blood plasma

Composition (mM)	Na^+	K^+	Mg^{2+}	Ca^{2+}	Cl^-	HPO_4^{2-}	SO_4^{2-}	HCO_3^-
SBF	142	5	1.5	2.5	147.8	1	0.5	4.2
Blood plasma	142	5	1.5	2.5	103.0	1	0.5	27.0

3.3. Cellular adhesion

The samples were introduced in Petri dishes, packed and sterilized by autoclaving at 121°C for 30 minutes.

Cell culture: Human osteoblast cells were maintained in a McCoy's culture medium supplemented with 10% inactivated bovine fetal serum, 50 U/ml penicillin, 50 mg/ml streptomycin, 1% L-glutamine. The cells were split every 2 days by a ratio of 1:3 and incubated at 37°C and 5% CO_2. All studies were done 72 hours after cell cultivation.

Cell adhesion: The samples were washed with phosphate buffer saline (PBS), fixed with 4% paraformaldehyde (20 min, 4°C), and permeabilised with 0.2% Triton X-100 for 3 min. Phosphate buffer saline (PBS) used for experiments was prepared by mixing 0.1 M phosphate buffer with 0.05 M NaCl, pH 7.0.

Actin filaments were labelled with Alexa Fluor 594 phalloidin (Invitrogen) and vinculin with anti-vinculin antibody (mouse monoclonal from Sigma) followed by Alexa Flour 488 goat anti-mouse antibody (Invitrogen). Vinculin and actin are local adhesion proteins present at contact points between cells and support surfaces. Vinculin connects adhesion receptors (integrins) with actin fibbers belonging to the cell cytoskeleton. Hence, the cell distribution of these proteins could offer useful information regarding the contact between osteoblasts and bioglass films.

Cells were mounted with Vectashield (Vector Laboratories Inc.) and visualized on Nikon Eclipse E600 fluorescence microscope.

4. Results and discussions

4.1. Scratch resistance and hardness

Two different titanium substrates, with irregularities (scratches, grooves, and protuberances), having $2.288 \cdot 10^{-6}$ m root mean square (RMS) roughness - named sample 1 and respectivelly $3.101 \cdot 10^{-6}$ m root mean square roughness - named sample 2, coated with PMMA+BG thin films having same thickness, were analysed in order to compare the scratch resistance of the film and the adhesion of the film on the substrate (see Fig. 1).

Three tests have been performed on each sample using the CSM Nano Scratch Tester.

Critical load – Lc – was defined as the normal load at which the delamination of the coating appears. In figure 2 we have a picture of this event taken on sample 1 ($RMS_{Ti} = 2.288 \cdot 10^{-6}$ m) and sample 2 ($RMS_{Ti} = 3.101 \cdot 10^{-6}$ m).

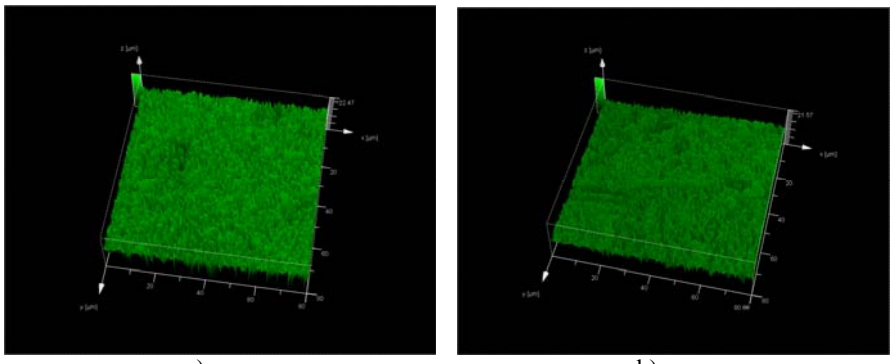

a) b)

Fig.1 CLSM images of : a) sample 1 and b) sample 2.
40X magnification, 0.7 aperture, 3.12 zoom

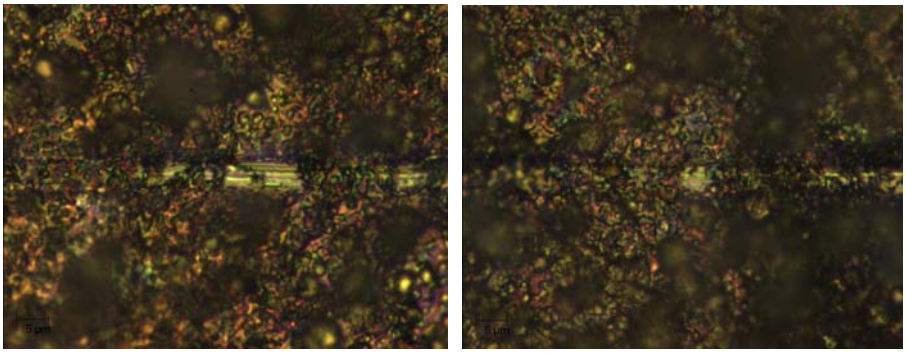

a) b)

Fig. 2 First delamination for: a) sample 1 and b) sample 2.

Table 2 illustrates the critical load values on each scratch per sample. Despite the high roughness of the samples, the results are very repeatable as they show the low value of standard deviation.The critical load founded for sample 2 is bigger than for sample 1 therefore the sample 2 has a better adhesion than the sample 1.

Table 2

The load values for the first delamination for samples

LC1 (10^{-3} N)	Sample 1	Sample 2
Data 1	36.25	48.31
Data 2	32.44	52.40
Data 3	28.12	56.21
Mean	***32.27***	***52.31***
Std. deviation	4.25	4.00

Therefore the use of the substrate with higher roughness provides coatings with better adhesion on the substrate, proper to biomedical applications. For further deposition of PMMA + BG thin films we used the titanium substrate with RMS_{Ti} =3.101·10^{-6} m root mean square roughness due to these considerations.
The investigated polymer-glass composite had hardness about 3000 MPa, so it is suitable as cover for bone implants [8].

4.2. Evaluation of bioactivity

We investigated bioactivity for two types of PMMA+BG films obtained from MAPLE targets which had a diferent PMMA/BG ratio: PMMA/BG=7.5 (named PMMA+BG 1) and PMMA/BG =5 (named PMMA+BG 2). The target for PMMA+BG 1 is made of 6•10^{-4} kg PMMA reinforced with 8•10^{-5} kg of 6P57 bioactive glass particles dissolved in 19.3•10^{-6} m^3 chloroform. For PMMA+BG 2 we used more bioactive glass, 6•10^{-4} kg PMMA reinforced with 12•10^{-5} kg of BG bioglass particles dissolved in 19.3 ·10^{-6} m^3 chloroform.

Figure 3 makes a comparison between the FTIR spectra in absorbance mode for these PMMA+BG structures deposited by the MAPLE technique. The FTIR spectra show diferent aspects. In the PMMA+BG 1 spectrum the peaks of PMMA prevail, such as a sharp intense peak at 1721·10^{-2} m^{-1} due to the presence of ester carbonyl group stretching vibration, the broad peak ranging form 1260-1000·10^{-2} m^{-1} owing to the C-O (ester bond) stretching vibration, the broad band from 950-650 ·10^{-2} m^{-1} due to the bending of C-H. In the PMMA+BG 2 spectrum the peaks of BG prevail, such as the peaks at 753·10^{-2} m^{-1}, 982 ·10^{-2} m^{-1} and 1008·10^{-2} m^{-1} belonging to Si-O bending vibration modes.

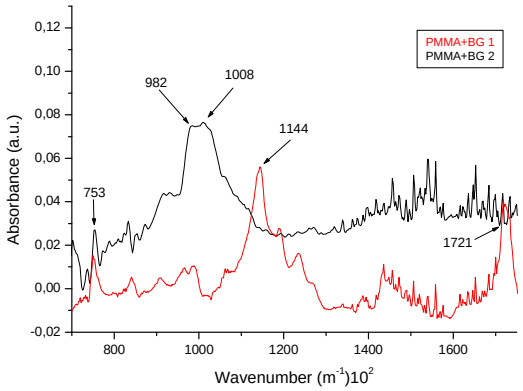

Fig 3. FTIR spectra of PMMA+BG 1 (bottom) and PMMA+BG 2 (top)

A lot of both PMMA+BG 1 and 2 samples were immersed into SBF and extracted after one day, one week and two weeks then analysed by FTIR. The sample presented a different behavior.

After one day of immersion into SBF solution, in the case of both PMMA+BG 1 and 2 samples, we can notice the growth of amplitude for all peaks (see Fig. 4) that indicates the forming of a rich superficial layer, where all elements have a greater concentration. This is consistent with other experimental observations made for bioactive glassbioactive glasses [9,10] and it is accompanied by the loss of soluble silica into the solution, fact emphasized by the depreciation of the surface's quality observed by surface morphology analysis (see 4.3).

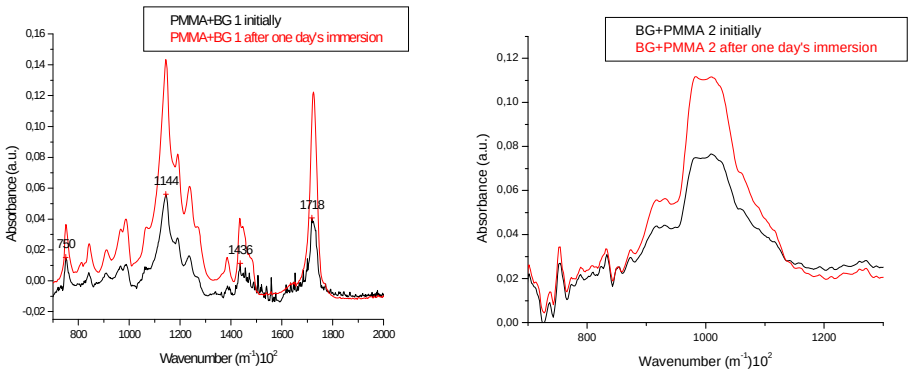

a) b)

Fig.4 FTIR spectra of PMMA+BG1 (a) and PMMA+BG 2 (b) films before and after one day of immersion into SBF

After oneweek of immersion into SBF, spectrum of PMMA+BG 1 samples does not change (see Fig. 5a), while major transformations can be clearly noticed on the surface of the coatings PMMA+BG 2 (see Fig. 5b): the bioactive glass peaks from $982 \cdot 10^{-2}$ m^{-1} and $1008 \cdot 10^{-2}$ m^{-1} decrease and a new peak appears, at $1034 \cdot 10^{-2}$ m^{-1} that belongs to asymmetric stretching of P-O bond of $(PO_4)^{3-}$. This indicates diminishing silica concentration and appeareance of the hydroxyapatite on surface coating.

Referring to figure 6 in a typical FTIR scan of PMMA+BG 1 immersed for two weeks we could notice very little changes in the peaks' amplitude: peaks of PMMA+BG decreased $-1144 \cdot 10^{-2}$ m^{-1} and $1722 \cdot 10^{-2}$ m^{-1} decreased and the other peaks at 633, 960, 1076 and $1470 \cdot 10^{-2}$ m^{-1}; these little peaks are assigned of hydroxyapatite and indicate that the process of hydroxyapatite appearance is beginning.

On the other hand in the case of the PMMA+BG 2 coatings, the corresponding peaks for hydroxyapatite are well emphasized at 630, 865, 961, 1031 and $1090 \cdot 10^{-2}$ m^{-1} . They correspond to asymmetric (peaks at 1031 and $1090 \cdot 10^{-2}$ m^{-1}) and respective symmetric (peak at $961 \cdot 10^{-2}$ m^{-1}) stretching of P– O bond in $(PO_4)^{3-}$, to $(HPO_4)^{2-}$ replacing the $(PO_4)^{3-}$ (peak at $865 \cdot 10^{-2}$ m^{-1}) and also to the vibrational mode of OH (peak at $630 \cdot 10^{-2}$ m^{-1}). At the same time the peaks belonging to bioactive glass disappear.

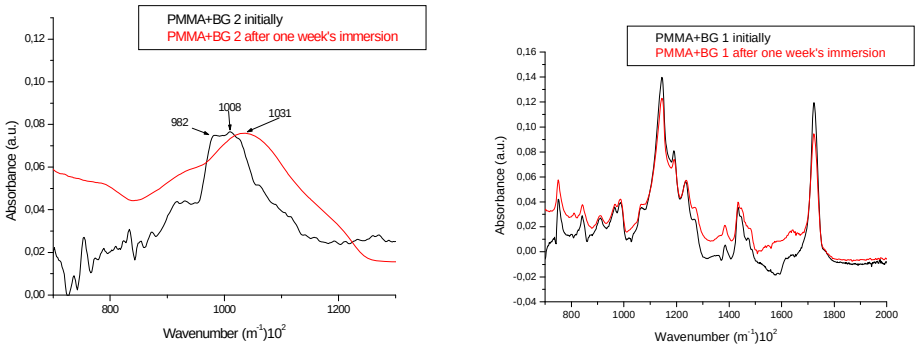

a) b)

Fig..5 FTIR spectra of PMMA+BG1 (a) and PMMA+BG 2 (b) film before and after one week of immersion into SBF

These certify two things: the disolution of the bioactive glass and the existence on the surface of a freshly growing carbonated hydroxyapatite $Ca_{8.3}(PO_4)_{4.3}(HPO_4,CO_3)_{1.7}(OH,CO_3)_{0.3}$, which is the predominant mineral component of vertebrate bones. This growth of hydroxyapatite layer demonstrates the ability of the polymer-bioglass composite to achieve firmly bound to tissues through a chemical bond at the bone/implant interface.

This behavior is similar to that reported for bulk glasses in the SiO_2-Na_2O-K_2O-CaO-MgO-P_2O_5 system, immersed into SBF [11-14], and it is in accordance with the mechanism of apatite formation described by Hench for bioactive glassbioactive glasses [10]. The proposed subsequent steps were: i) the exchange of Na^+ and K^+ from glass with H^+ or H_3O^+ from SBF, accompanied by the loss of soluble silica into the solution and the formation of silanols (Si-OH) on the glass surface; ii) condensation and repolymerization on surface of the SiO_2^--rich layer; iii) migration of Ca^{2+} and PO_4^{3-} though the silica-rich layer forming a CaO-P_2O_5 -rich film that incorporates calcium and phosphates from solution, and iv) the crystallization of the amorphous calcium phosphate film to form an apatite layer.

However the bioactivity of material is lower than that of pure bioactive glass BG films [15,16] where the growing carbonated hydroxyapatite begins

earlier, after few days of immersion. PMMA additions reduce the bone bonding ability of bioactive glasses; this is in agreement whith the studies of the effect of other materials introduction in bioactive glasses published by Ohura et al. [17] and Anderson et al. [18]. PMMA+BG 2 films have more bioactive glass than

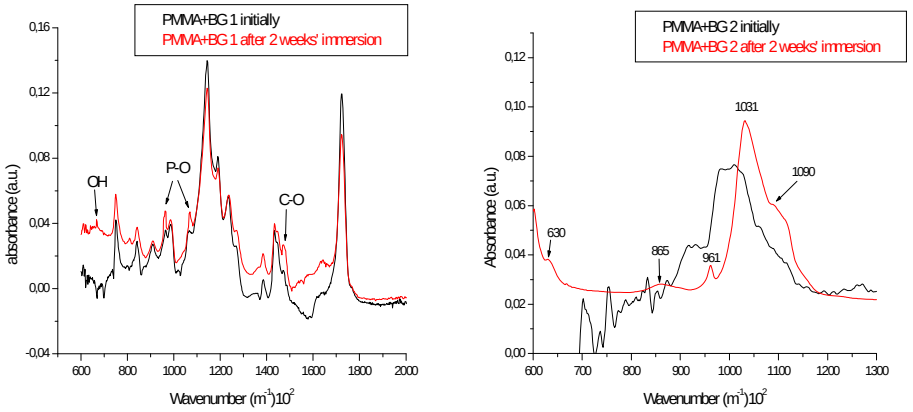

a) b)

Fig..6 FTIR spectra of PMMA+BG 1 (a) and PMMA+BG 2 (b) films before and after two weeks of immersion into SBF.

PMMA+BG 1 and are more bioactive; for BG+PMMA 2 films a hydroxyapatite layer is partially formed after oneweek of immersion into SBF, while for PMMA+BG 1 it is not visible until after the two weeks of immersion.

4.3. Surface morphology of PMMA+BG films

Subsequently we have examined carefully the surface morfology of PMMA+BG 2 bioactive films before and after one week and two weeks of immersion into simulated body fluid.

3D image of titanium substrate (see Fig.7a) revealed the structure with a characteristic configuration, consisting of a great number of irregularities and having $3.101 \cdot 10^{-6}$ m root mean square roughness.

The coating deposited from cryogenic targets of PMMA+BG 2 on the titanium substrate preserved his morphology (see Fig. 7 b) but the film surface had greater irregularities and its root mean square roughness became RMS=$3.813 \cdot 10^{-6}$ m, a value suitable for orthopedic applications, known for the fact that for these the perfect roughness is less than 1 millimeter. Such feature favors biocompatibility which significantly increases with the specific area of the

deposited biofilms. Indeed, the rougher the area due to surface protuberances, the higher the proliferation of viable cell cultures is [19,20].

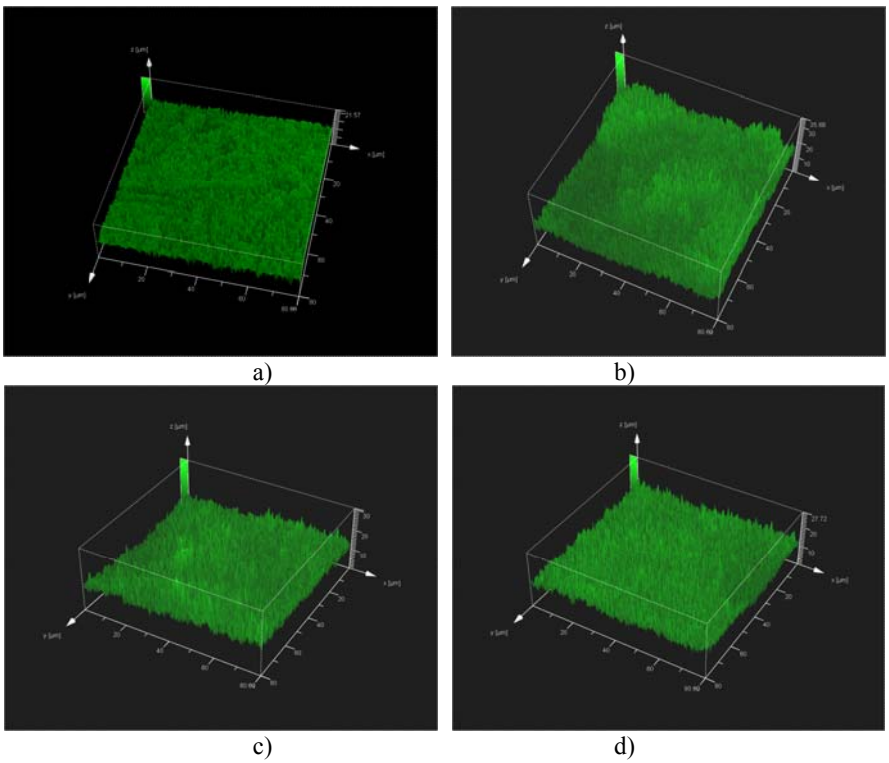

Fig.7 3D images (40X magnification, 0.7 aperture, 3.12 zoom) for: a) titanium substrate, b) PMMA+BG 2 initial film, c) PMMA+BG 2 film after 1 week of immersion into SBF, d) PMMA+BG 2 film after 2 weeks of immersion into SBF

After one week of immersion the bioactive glass from bioactive film was dissolved in SBF and the root mean square roughness of surface decreased down to RMS=$2.726 \cdot 10^{-6}$ m. Thus 3D image (see Fig. 7 c) and topographical image (see Fig. 8 c) support observations by FTIR (see Fig 5 b).

FTIR analyzes certify the continuation of the bioactive glass dissolution and the appearance on the surface of a freshly growing carbonated hydroxyapatite after twoweeks of immersion into SBF and CLSM confirms these affirmations: in figures 7d and 8d we can see new particules of variable size in the micrometric range that are randomly distributed over the whole investigated area. Surface root mean square roughness still diminishes and becomes RMS=$2.308 \cdot 10^{-6}$ m.

One advantage of PMMA+BG structure over bioactive glass films which makes it so great for implantology is that PMMA does not dissolve in SBF but remains on the substrate and in this way implant corrosion and the release of

metallic ions into the body are prevented, at the same time the structure preserves the bioactive glass bioactivity.

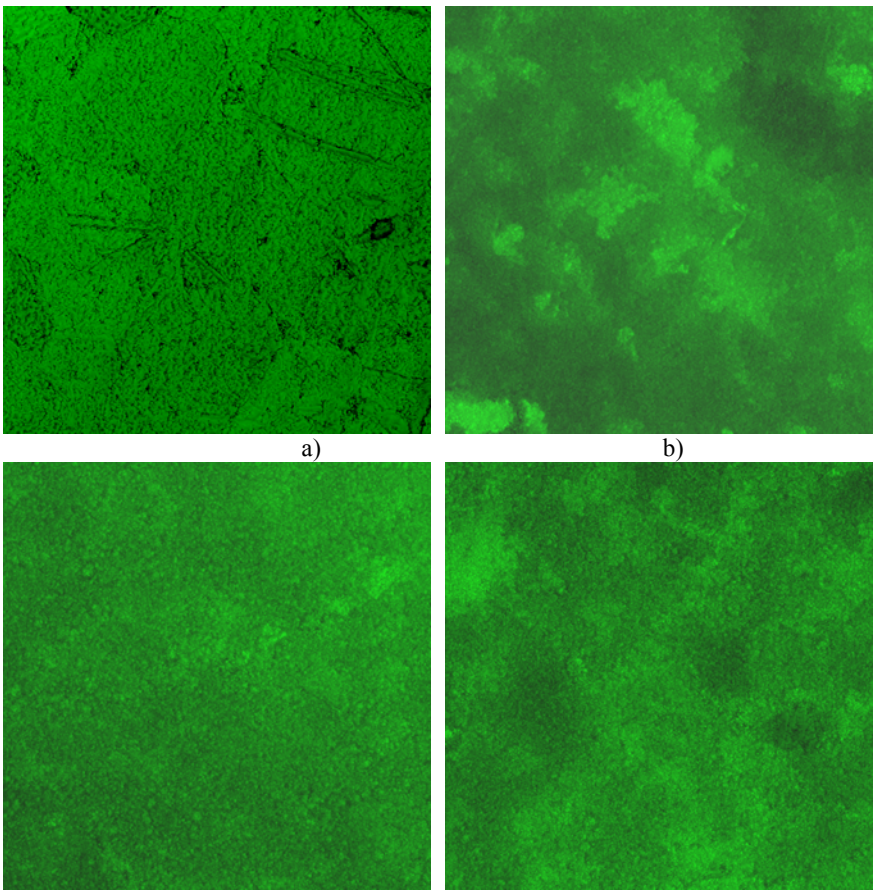

Fig.8 Topography (40X magnification, 0.7 aperture, 1 zoom) for: a) titanium substrate, b) PMMA+BG 2 initial film, c) PMMA+BG 2 film after 1 week of immersion into SBF, d) PMMA+BG 2 film after 2 weeks of immersion into SBF.

In order to validate this claim we have investigated the resistance at corrosion of the polymer - bioactive glass both used as coatings for implants or prosthesis on Ti substrate, using electrochemical methods, the most used methods because of their high sensibility. Potentiodynamic polarization studies show that these structures exhibit higher corrosion resistance compared to bare titanium. The hydroxyapatite (HA) layer that grows on the titanium implant surface after his introduction into human body presents also a good protection for implant. The behaviour of the studied coatings into contact with physiological fluids was found in vitro by electrochemical impedance spectroscopy. The initial coating of

bioglass-polymer is a good insulator, but after some days of immersion into physiological fluids two processes are happening at the same time: the bioglass dissolution and the adsorption of some electrolyte ions, that determines the formation of a new liquid – layer interface and finally an outer protective layer which facilitates the osseointegration [21]. Thus titanium implant is tied to bone through these insulator layers, it does not come in direct contact with physiological fluids.

4.4. Evaluation of cell attachment

The primary osteoblasts grown on PMMA+BG were visualized with a fluorescence microscope (Fig.9). The staining of the two interesting proteins was made with fluorescent marks visualised on green channel for vinculin and respective red channel for actin. Cells' nuclei were stained with DAPI and they were visualised on blue channel of fluorescence. The overlap of images shows the spatial localization of vinculin and actin on the film surfaces, with some co-localization of vinculin with actin filaments ends. This may suggest that vinculin was activated and was able to induce the generation of focal adhesion points.

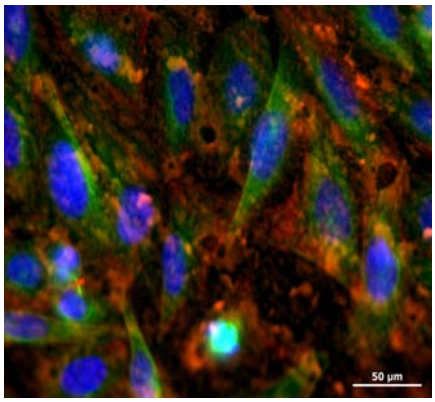

Fig. 9 Fluorescence image of PBG2 film surface: green staining of vinculin, red staining of actin and blue staining of nuclei in cells cultured on the film surface after 3 days of culture

The osteoblasts are well spread out on the polymer-bioglass films, with numerous contact points with the bioglass surface, indicating a good cell adhesion. The actin filaments are well highlighted in all cells and evidence the cytoskeleton organization. The cells present an irregular disposal due to the irregular surface of the film, with the pseudopods infiltrating into the depth of the material which increase adhesion. They are well spread out and attached to the film on a large surface. This is an evidence of the films biocompatibility.

Unfortunatelly, both the polymer and the bioglass show a high degree of self-fluorescence, on both the red channel and the green one, and this hinders the obtaining of very good photos.

5. Conclusions

We have reported the performance of PMMA+BG thin films by the matrix assisted pulsed laser evaporation technique, deposition made with preservation of the basic materials stoichiometry.
We have found from mechanical tests that these composite films provide a better adhesion on the substrate and a better hardness for application in implantology. We have tested the obtained films in simulated body fluid solution and we have validated their bioactivity. When they are in contact with body fluids, the films present the ability to stimulate the growth of hydroxyapatite on their surface what demonstrates the ability of the polymer-bioglass composite to achieve firmly bound to tissues through a chemical bond at the bone/implant interface. Interaction between human osteoblasts and tested materials was studied by fluorescent mark of cellular proteins: actin and vinculin. The human osteoblasts were shown to cover entirely the structures with which they strongly interact, as proved by the pseudopodia deeply infiltrating into the composite material.

We can conclude that PMMA+BG compositions are suitable for being used as coatings on biological implants and they allow stable fixation to bone. PMMA+BG deposited by the matrix assisted pulsed laser evaporation technique on the titanuim substrate may be first nanostructure of a new generation of implants.

Acknowledgements

We are grateful to Mihaela Voinea and Daniel Munteanu (Transilvania University of Brasov), Roxana Mustata and Livia Sima (Institute of Biochemistry of Romanian Academy, Bucharest Romania) for their support and precious help regarding FTIR measurements, scratch tests and cell attachement respectively.

R E F E R E N C E S

[1] *L. L. Hench, E.C. Ethridge*, Biomaterials, An Interfacial Approach, Academic Press, New York, 1982
[2] *L.L.Hench, O. Andersoon*, Bioactive glass coatings, in Hench LL, Wilson J, editors, An introduction to bioceramics, New Jersey, World Scientific, 1993, pp. 239-260

[3] *S.R. Sousa, M.A. Barbosa*, Effect of hydroxyapatite thickness on metal ion release from Ti6Al4V substrates, in Biomaterials, **vol. 17**, 1996, 397–404
[4] *T. Kokubo*, Proceedings of the Third Euro-Ceramics, in Faenza Editrice Iberica, San Vincente, 1993, **vol. 3,** 1993
[5] *J. D. Santos, P. L. Silva, J.C. Knowles, S. Talal, F. J. Monteiro,* Reinforcement of hydroxyapatite by adding P2O5-CaO glasses with Na2O, K2O and MgO, in J. Mater. Sci., Mater Med., **vol. 7**, 1996, pp. 187-189
[6] *S.N. Salama, H. Darwish, H.A. Abo-Mosallam*, Crystallization and properties of glasses based on diopside–Ca-Tschermak's–fluorapatite system, J. Eur. Ceram. Soc., **vol. 25,** 2005, pp. 1133–1142
[7] *T. Kokubo, H. Kushitani, S. Sakka, T. Kitsugi, T. Yamamuro*, Solutions able to reproduce in vivo surface-structure changes in bioactive glass-ceramic A-W3, in J. Biomed. Mater. Res., v**ol. 24**, 1990, pp. 721-734
[8] *R. Teghil, L. D'Alessio, D. Ferro, S. M. Barinov,* Hardness of bioactive glass film deposited on titanium alloy by pulsed laser, in J. Mater. Sci. lett., **vol 21**, 2002, pp. 379– 382
[9] *E. Saiz, A.P. Tomsia, A. Pazo*, Silicate glass coatings on Ti-based implants, in Acta Mater, **vol. 46**, 1998, pp. 2551-2558
[10] *L .L. Hench*, Bioceramics: from concept to clinic, in J. Am. Ceram.Soc., **vol. 74**, 1991, pp. 1487-1510
[11] *M. Ogino, F. Ohuchi, L.L. Hench*, Compositional dependence of the formation of calcium phosphate films on bioglass, in J Biomed Mater Res., **vol. 14**, 1980, pp. 55-64
[12] *R. Hill*, An alternative view of the degradation of bioglass, in J Mater Sci Lett, **vol. 15**, 1996, pp. 1122-1125
[13] *J.M. Gomez-Vega, E. Saiz, AP. Tomsia*, Glass-based coatings for titanium implant alloys, in J Biomed Mater Res., **vol.46,** 1999, pp. 549-559
[14] *E. Saiz, A.P. Tomsia, A. Pazo*, Bioactive coatings on Ti and Ti6Al4V alloys for medical applications, in: Tomsia AP, Glaeser AM, (Eds), Ceramic microstructures: control at the atomic level, Berkeley, Plenum Press, 1998, pp. 543–550
[15] *L. Floroian, B. Savu, F. Sima, I. N. Mihailescu, D. Tanaskovic, D. Janackovic*, Synthesis and characterisation of bioglass thin films, in Digest Journal of Nanomat. And Biostrustures, **vol. 2**, 2007, pp. 285-291
[16] *L. Floroian, B. Savu, G. Stanciu, A. C. Popescu, F. Sima, I.N. Mihailescu, R. Mustata, L.E.Sima, S.M. Petrescu, D. Tanaskovic, Dj. Janackovic*, Nanostructured bioglass thin films syntherized by pulsed laser deposition: CLSM, FTIR investigations and in vitro biotests, in Applied Surface Science, 2008, **vol. 255**, pp. 3056-3062
[17] *K. Ohura, T. Nakamura, T. Yamamuro, Y. Ebisawa, T. Kokubo, Y. Kotoura, M. Oka*, Bioactivity of CaO SiO2 glasses added with various ions, in J Mater Sci, **vol. 3**, 1992, pp. 95-100
[18] *O.H. Andersson, K.H. Karlsson, K. Kangasniemi, A. Yli- Urpo*, Models for physical properties and bioactivity of phosphate opal glasses, in Glastech Ber, **vol. 61**, 1988, pp. 300-305
[19] *D.M. Bubb, R.F. Haglund Jr.,* Resonant infrared pulsed laser ablation and deposition of thin polymer films, in: R. Eason (Ed.), Pulsed Laser Deposition of Thin Films: Applications-Lead Growth of Functional Materials, Wiley & Sons, New York, USA, 2006, pp. 35-61.

[20] *V. Nelea, C. Morosanu, M. Iliescu, I.N. Mihailescu*, Hydroxyapatite thin films grown by pulsed laser deposition and radio-frequency magnetron sputtering: comparative study, in Appl. Surf. Sci., **vol. 228,** 2004, pp. 346–356.
[21] *L. Floroian, I.N. Mihailescu, F. Sima, R. Cristescu, M. Florescu, M. Badea,* Electrochemical behaviour evaluation of bioglass-polymer nanocomposite for biomedical applications, in press